CANCER BIOTHERAPY AND RADIOPHARMACEUTICALS
Volume 32, Number 8, 2017
Mary Ann Liebert, Inc.
DOI: 10.1089/cbr.2017.2233

Imaging of Integrin $\alpha_v\beta_3$ Expression in Lung Cancers and Brain Tumors Using Single-Photon Emission Computed Tomography with a Novel Radiotracer ^{99m}Tc-IDA-D-[c(RGDfK)]$_2$

Yoo Sung Song,[1,*] Hyun Soo Park,[1,2,*] Byung Chul Lee,[1,3]
Jae Ho Jung,[1] Ho-Young Lee,[1] and Sang Eun Kim[1–3]

Abstract

Integrin $\alpha_v\beta_3$ is a molecular marker for the estimation of tumor angiogenesis and is an imaging target for radiolabeled Arg-Gly-Asp (RGD) peptides. In this study, the authors investigated the clinical efficacy and safety of a novel radiolabeled RGD peptide, ^{99m}Tc-IDA-D-[c(RGDfK)]$_2$, for the imaging of integrin $\alpha_v\beta_3$ expression, as a measure of tumor angiogenesis in lung cancers and brain tumors. Five patients with lung cancers and seven with brain tumors underwent ^{99m}Tc-IDA-D-[c(RGDfK)]$_2$ single-photon emission computed tomography (SPECT) imaging. Tumors were also assessed using ^{18}F-fluorodeoxyglucose positron emission tomography/computed tomography. Uptake of the radiotracer was expressed as the tumor-to-normal uptake ratio (TNR). All the lung cancers and brain tumors were well visualized on ^{99m}Tc-IDA-D-[c(RGDfK)]$_2$ SPECT. TNR for ^{99m}Tc-IDA-D-[c(RGDfK)]$_2$ was significantly higher than that for ^{18}F-FDG in brain tumors (6.4 ± 4.1 vs. 0.9 ± 0.4). Proliferation index of brain tumors showed a significant positive correlation with TNR for ^{99m}Tc-IDA-D-[c(RGDfK)]$_2$ and ^{18}F-FDG. No laboratory and clinical adverse events were reported after ^{99m}Tc-IDA-D-[c(RGDfK)]$_2$ injection. Their results suggest that ^{99m}Tc-IDA-D-[c(RGDfK)]$_2$ is an efficacious and safe radiotracer for imaging integrin $\alpha_v\beta_3$ expression with potential application to monitoring the clinical efficacy of antiangiogenic agents in malignant tumors. In addition, this is the first clinical application of radiolabeled RGD peptides for SPECT imaging of brain tumors.

Keywords: ^{99m}Tc-IDA-D-[c(RGDfK)]$_2$, brain tumor, integrin $\alpha_v\beta_3$ expression, lung cancer, single-photon emission computed tomography

Introduction

Angiogenesis is the process of new blood vessel formation from the preexisting vasculature. It is well accepted as a biomarker for the growth, invasion, and metastasis of numerous solid tumors.[1–3] Currently, there is a growing demand for novel noninvasive *in vivo* imaging techniques available for response assessment and pretherapeutic stratification of patients receiving antiangiogenic therapies. It has been suggested that angiogenesis-targeted imaging can provide an early diagnosis and aid in treatment planning and monitoring of antiangiogenic cancer therapies.[4–6]

Integrin $\alpha_v\beta_3$ is a suitable target for both tumor angiogenesis imaging and antiangiogenic therapy due to its high expression on activated endothelial cells and new blood vessels found in tumors and surrounding tissues, while absent in most intact

[1]Department of Nuclear Medicine, Seoul National University Bundang Hospital, Seoul National University College of Medicine, Seoul, Republic of Korea.
[2]Department of Transdisciplinary Studies, Graduate School of Convergence Science and Technology, Seoul National University, Seoul, Republic of Korea.
[3]Center for Nanomolecular Imaging and Innovative Drug Development, Advanced Institutes of Convergence Technology, Suwon, Republic of Korea.
*These authors contributed equally to this work.

© Yoo Sung Song et al. 2017; Published by Mary Ann Liebert, Inc. This article is available under the Creative Commons License CC-BY-NC (http://creativecommons.org/licenses/by-nc/4.0). This license permits non-commercial use, distribution and reproduction in any medium, provided the original work is properly cited. Permission only needs to be obtained for commercial use and can be done via RightsLink.

Address correspondence to: Sang Eun Kim; Department of Nuclear Medicine, Seoul National University Bundang Hospital; 300 Gumi-dong, Bundang-gu, Seoul 13620, Republic of Korea
E-mail: **kse@snu.ac.kr**

normal tissues.[7,8] Therefore, integrin $\alpha_v\beta_3$ is considered an indicator of activated angiogenesis; imaging of integrin $\alpha_v\beta_3$ overexpression is a promising technique for the assessment of angiogenesis.[9–11] Labeled synthetic ligands with demonstrated specificity for integrin $\alpha_v\beta_3$ have proven as successful agents for *in vivo* imaging of tumor angiogenesis.[4] In particular, agents based on the amino acid sequence Arg-Gly-Asp (RGD) have been identified as useful for tumor angiogenesis imaging.[12–14] A significant correlation between tracer uptake and the level of angiogenesis has been demonstrated in clinical *in vivo* studies of tumor imaging performed using radiolabeled RGD peptides.[15,16]

IDA-D-[c(RGDfK)]$_2$ is a newly developed, cyclic synthetic ligand containing the RGD binding site, with a high affinity ($IC_{50} = 50$ nM) for integrin $\alpha_v\beta_3$ during angiogenesis.[17] The IDA (iminodiacetate, $^{99m}Tc(CO)_3$) is suggested to have a better biodistribution with higher integrin $\alpha_v\beta_3$ tumor uptake compared with previous radiolabeled RGD peptides, due to its negative charge in the ^{99m}Tc core.[17,18] Preclinical imaging studies using ^{99m}Tc-labeled IDA-D-[c(RGDfK)]$_2$ (^{99m}Tc-IDA-D-[c(RGDfK)]$_2$) single-photon emission computed tomography (SPECT) demonstrated substantial and specific uptake of the radiotracer at the location of integrin $\alpha_v\beta_3$ overexpression in tumors,[17] as well as high-risk atherosclerotic plaques.[19] These previous studies demonstrated that the uptake of ^{99m}Tc-IDA-D-[c(RGDfK)]$_2$ correlated with the expression of integrin α_v or integrin β_3 in endothelial cells. In addition, ^{99m}Tc-labeled RGD peptides offer some advantages compared to previous ^{18}F or ^{68}Ga labeled RGD peptides. ^{99m}Tc-labeled peptides are more inexpensive, and the substitution of ^{99m}Tc with β-emitting ^{188}Re has the potential for therapeutic application.[17] Thus, ^{99m}Tc-IDA-D-[c(RGDfK)]$_2$ SPECT is a potential tool for *in vivo* assessment of angiogenesis through the visualization of integrin $\alpha_v\beta_3$ overexpression in solid tumors.

In the present study, the authors investigated the clinical efficacy of ^{99m}Tc-IDA-D-[c(RGDfK)]$_2$ for the SPECT imaging of integrin $\alpha_v\beta_3$ expression, as a measure of tumor angiogenesis, in lung cancers and brain tumors, which are among the representative tumors that overexpress integrin $\alpha_v\beta_3$.[20,21] The authors also compared ^{99m}Tc-IDA-D-[c(RGDfK)]$_2$ uptake with that of ^{18}F-fluorodeoxyglucose (FDG) as a measure of tumor glucose metabolism using positron emission tomography (PET), as a reference for tumor glucose metabolism to correlate integrin $\alpha_v\beta_3$ expression with tumor aggressiveness. Finally, the authors assessed the safety profile of ^{99m}Tc-IDA-D-[c(RGDfK)]$_2$.

Materials and Methods

Patients

Five patients (M:F = 4:1, 63.6 ± 6.2 years) with lung cancers (adenocarcinoma [$n = 3$], squamous cell carcinoma [$n = 1$], sarcomatoid carcinoma [$n = 1$]) and seven patients (M:F = 3:4, 64.7 ± 6.8 years) with brain tumors (glioblastoma [$n = 4$], anaplastic astrocytoma [$n = 1$], meningioma [$n = 1$], and metastatic adenocarcinoma [$n = 1$]) were recruited for the present study. The patient characteristics and staging/grading are presented in Table 1. The inclusion criteria were as follows: patients with histologically proven lung cancers or brain tumors, complete clinical staging, available computed tomography (CT), T_2-weighted magnetic resonance imaging (MRI), and/or ^{18}F-FDG PET/CT data, age >20 years, and the absence of pregnancy and impaired renal and hepatic function. Clinical outcome of lung cancer patients were verified using CT, according to response evaluation criteria in solid tumors as complete response (CR), partial response, stable disease (SD), and progressive disease (PD). Brain tumor patients were verified using MRI.

The present study was approved by the Institutional Review Board of the Seoul National University Bundang Hospital (IRB No.: B-1112-069-004). Informed consent was obtained from all individual participants included in the study. All procedures performed in studies involving human participants were in accordance with the ethical standards of the institutional research committee and with the 1964 Helsinki declaration and its later amendments or comparable ethical standards.

Synthesis of ^{99m}Tc-IDA-D-[c(RGDfK)]$_2$

The precursor was generously provided by Bio Imaging Korea Co., Ltd. (Seoul, Republic of Korea), which owns the intellectual property rights. Sodium pertechnetate (^{99m}Tc) was eluted on a daily basis from ^{99}Mo/^{99m}Tc-generator (Samyoung Unitech, Seoul, Republic of Korea). ^{99m}Tc-IDA-D-[c(RGDfK)]$_2$ was synthesized following the method described in their previous work.[17] A

Table 1. Patient Characteristics

Group	*Patient no.*	*Sex (M/F)*	*Age (years)*	*Pathology*	*TNM staging/WHO grade*
Lung cancer ($n = 5$)	1	M	65	Adenocarcinoma	T2bN2M1 (IV)
	2	F	67	Adenocarcinoma	T1bN1M0 (IIA)
	3	M	64	Adenocarcinoma	T1bN0M0 (IA)
	4	M	69	Squamous cell carcinoma	T1bN0M0 (IA)
	5	M	53	Sarcomatoid carcinoma	T2bN0M0 (IIA)
Brain tumor ($n = 7$)	6	F	71	Glioblastoma	IV
	7	F	69	Glioblastoma	IV
	8	F	75	Glioblastoma	IV
	9	F	59	Glioblastoma	IV
	10	M	62	Anaplastic astrocytoma	III
	11	M	59	Meningioma	I
	12	M	58	Metastasis (lung, adenocarcinoma)	

F, female; M, male; TNM, tumor, node, and metastasis.

solution of $[^{99m}Tc(H_2O)_3(CO)_3]^+$ (370–740 MBq) in saline (200 μL), which was prepared according to the protocol described by Alberto et al.,[22] was added to the precursor in water (300 μL). After stirring of the reaction mixture at 75°C for 30 minutes, the obtained ^{99m}Tc-IDA-D-[c(RGDfK)]$_2$ was purified by semipreparative high-performance liquid chromatography (HPLC; Eclipse XDB-C18 column; 5 mm, 9.4 × 250 mm; Agilent Co., Palo Alto, CA), and a 214 nm UV detector was used for monitoring the effluent from the column, which was followed by a gamma radioactive detector. The same gradient conditions are described in their method. Products isolated from semipreparative HPLC were diluted with excess water and were passed through a tC18 Sep-Pak cartridge and washed with water (5 mL). The final product was eluted by 80% ethanol–saline (1.5 mL) and evaporated by a stream of nitrogen gas. Dissolvement in saline and sterile filtering (0.22 μm) was done for injection preparation. All radiochemical processes, including Tc-99 m incorporation, HPLC purification, and tC_{18} Sep-Pak cartridge purification, were conducted within 60 ± 5 minutes. A quality control check with pH, endotoxin testing, analytic HPLC, and residual solvent measurement by gas chromatography was performed before human injection; a radiochemical purity of 95% was mandatory.

^{99m}Tc-IDA-D-[c(RGDfK)]$_2$ SPECT

^{99m}Tc-IDA-D-[c(RGDfK)]$_2$ SPECT imaging was performed using a dual-head Forte system (Philips Medical Systems, Cleveland, OH) for patients with lung cancers and a triple-head TRIAD system (Trionix Research Laboratory, Twinsburg, OH) for patients with brain tumors. Both SPECT scanners were calibrated for Bq/mL by imaging a phantom with known activity determined by a dose calibrator before the study. Patients were placed in the SPECT scanner in a head-first supine position and were intravenously injected with 260–370 MBq of ^{99m}Tc-IDA-D-[c(RGDfK)]$_2$ for brain tumor patients and 555–740 MBq of ^{99m}Tc-IDA-D-[c(RGDfK)]$_2$ in 10 mL of sterile saline for lung cancer patients. Injection administered doses were determined according to the previous references of other ^{99m}Tc-labeled RGD peptides.[23–25] Specific activity of ^{99m}Tc-IDA-D-[c(RGDfK)]$_2$ was 110–220 MBq/nmol, which was obtained after purification in an HPLC column. Images were acquired 30 minutes after injection. SPECT acquisitions were performed using a 360° circular orbit detector rotation for 30 minutes (number of rotation = 1, 90 frames of 4° angular step [45 steps per detector], each of 40 seconds), by a step and shoot method. Energy window was set at minimum 124–maximum 151 KeV. For lung cancers, image was reconstructed using filtered back projection method with Butterworth filter. Image matrix was 128 × 128 voxels of 3.44 × 3.44 mm^2 with 3.44 mm slice thickness. For brain tumor, image was zoomed with a factor of 2.0 and was reconstructed using filtered back projection method with Butterworth filter. The attenuation correction coefficient was set at 0.110. Image matrix was 128 × 128 voxels of 1.78 × 1.78 mm^2 with 1.78 mm slice thickness.

^{18}F-fluorodeoxyglucose PET/CT

^{18}F-FDG PET/CT was performed using a Discovery VCT PET scanner (GE Healthcare, Milwaukee, WI). All ^{18}F-FDG PET/CT was performed within 1 day of ^{99m}Tc-IDA-D-[c(RGDfK)]$_2$ SPECT imaging. The PET scanner was calibrated for Bq/mL by imaging a phantom with known activity determined by a dose calibrator before the study. Patients were instructed to fast for at least 6 hours before scanning. PET images were obtained with patients in the head-first supine position 50 minutes after intravenous injection of ^{18}F-FDG (5.18 MBq/kg), after fasting for at least 6 hours. PET images were acquired in a three-dimensional acquisition mode (1 bed position for brain tumor, 5–6 bed position for lung cancer, 2.5 minutes/bed) and were reconstructed on 128 × 128 matrices using an iterative algorithm (ordered subset expectation maximization, 2 iterations and 8 subsets). CT images (120 kVp, 3.75 mm slice thickness) were acquired for CT-based attenuation correction.

Image analysis

All acquired images were processed using the comprehensive image analysis software package PMOD (version 3.13, PMOD Technologies, Inc., Zurich, Switzerland). For ^{18}F-FDG PET, standardized uptake value (SUV) was calculated using the following formula: [measured activity concentration (Bq/mL) × body weight (g)/injected activity (Bq/mL)]. ^{99m}Tc-IDA-D-[c(RGDfK)]$_2$ SPECT and ^{18}F-FDG PET images were automatically and/or manually coregistered to generate fusion images in the same matrix, with the same coordinates of the tumoral lesion across images. A tumor lesion was visually identified, and a volume of interest (VOI) encompassing the entire lesion was drawn on the basis of anatomical images (T_2-weighted MR image for brain tumors and CT image for lung cancers). A VOI with the same size and shape was drawn in the contralateral normal tissues for brain tumors. For lung cancers VOI with the same size and shape was drawn on the contralateral lobes (right upper lobe vs. left upper lobe, right middle lobe vs. left lingular lobe, right lower lobe vs. left lower lobe, respectively). The VOIs were used to obtain gamma counts for SPECT images and SUV values for PET images. Tumor-to-normal uptake ratio (TNR) was calculated as mean voxel value for the tumor VOI/mean voxel value for the contralateral VOI.[24]

Immunohistochemistry

Immunohistochemistry (IHC) staining and pathologic reports of the primary malignant brain tumors were reviewed. IHC testing was performed on an automated IHC stainer (BenchMark XT; Ventana Medical Systems, Inc., Tucson, AZ) for the examination of the Ki-67 proliferation index, loss of PTEN, and overexpression of the following proteins: GFAP, IDH-1, EGFR, and p53.

Safety assessment for ^{99m}Tc-IDA-D-[c(RGDfK)]$_2$

Patients' safety was assured throughout the whole procedure of ^{99m}Tc-IDA-D-[c(RGDfK)]$_2$ SPECT imaging. Safety assessment included adverse event reporting and evaluation of general appearance, vital signs (systolic and diastolic blood pressure, respiratory rate, heart rate, and body temperature), electrocardiogram, and physical and neurological examinations undertaken at various time points before, during, and after ^{99m}Tc-IDA-D-[c(RGDfK)]$_2$ administration and SPECT

imaging. All subjects were telephoned by an investigator 24 hours after ^{99m}Tc-IDA-D-[c(RGDfK)]$_2$ administration to question about the occurrence of possible adverse events.

Statistical analyses

All quantitative data are expressed as mean ± standard deviation. Mean values were compared with Wilcoxon signed-rank test. The correlation between quantitative values was evaluated using linear regression analysis and by calculation of Pearson's correlation coefficients (r). All statistical analyses were performed using Prism software (version 5; GraphPad Software, Inc., La Jolla, CA). The level of statistical significance was set at 5%.

Results

Safety profile of ^{99m}Tc-IDA-D-[c(RGDfK)]$_2$

None of the patients experienced an adverse event associated with ^{99m}Tc-IDA-D-[c(RGDfK)]$_2$ injection. No clinically important trends or safety signals in vital signs, laboratory parameters, electrocardiogram, and physical and neurological examinations were noted during the ^{99m}Tc-IDA-D-[c(RGDfK)]$_2$ SPECT imaging period. Related data are described in Supplementary Table S1 (Supplementary Data are available online at www.liebertpub.com/cbr).

Clinical response

Among lung cancer patients, one adenocarcinoma patient had PD and four other patients achieved CR. Among brain tumor patients, one meningioma patient achieved SD, and six other patients had PD. Clinical responses, overall survival, and progression-free survival are presented in Table 2.

Lung cancer

The tumor volumes (VOI size) in patients with lung cancers ranged from 3 to 176 mm^3. All lesions were well visualized on ^{99m}Tc-IDA-D-[c(RGDfK)]$_2$ SPECT images, with their locations corresponding to those on CT and ^{18}F-FDG PET/CT images (Fig. 1). The quantification results for ^{99m}Tc-IDA-D-[c(RGDfK)]$_2$ and ^{18}F-FDG PET/CT are shown in Table 2. The TNR for ^{99m}Tc-IDA-D-[c(RGDfK)]$_2$ images ranged from 1.0 to 3.5. The SUV for ^{18}F-FDG PET/CT images ranged from 1.4 to 7.4, with TNR from 2.0 to 18.7. There was no statistically significant difference in TNR values on ^{99m}Tc-IDA-D-[c(RGDfK)]$_2$ SPECT images and ^{18}F-FDG PET/CT images ($p = 0.06$) (Fig. 2a). The correlation between the TNRs of ^{99m}Tc-IDA-D-[c(RGDfK)]$_2$ SPECT and ^{8}F-FDG PET/CT images was marginal ($r = 0.85$, $p = 0.06$). Among the adenocarcinoma patients, the one patient who had PD had the highest TNR of ^{99m}Tc-IDA-D-[c(RGDfK)]$_2$ (patient no. 2).

Brain tumor

The tumor volumes in patients with brain tumors ranged from 2 to 65 mm^3. All lesions were well visualized on ^{99m}Tc-IDA-D-[c(RGDfK)]$_2$ SPECT images, with their locations corresponding to those on T_2-weighted MR and ^{18}F-FDG PET images (Fig. 3). The quantification results for ^{99m}Tc-IDA-D-[c(RGDfK)]$_2$ and ^{18}F-FDG PET/CT are shown in Table 2. The TNR for ^{99m}Tc-IDA-D-[c(RGDfK)]$_2$ images ranged from 2.2 to 13.8. The SUV for ^{18}F-FDG PET/CT images ranged from 2.9 to 7.1, with TNR from 0.4 to 1.3. Tumor contrast was more prominent on ^{99m}Tc-IDA-D-[c(RGDfK)]$_2$ SPECT images than on^{18}F-FDG PET/CT images. TNR values of ^{99m}Tc-IDA-D-[c(RGDfK)]$_2$ SPECT images were significantly higher than those on ^{18}F-FDG PET/CT images ($p = 0.02$) (Fig. 2b). Grade IV glioblastoma patients had higher TNR values of ^{99m}Tc-IDA-D-[c(RGDfK)]$_2$ SPECT images compared with grade III anaplastic astrocytoma and grade I meningioma patient. There was no significant correlation between the TNRs on ^{99m}Tc-IDA-D-[c(RGDfK)]$_2$ SPECT and ^{8}F-FDG PET/CT images.

IHC of brain tumor

IHC results of five primary malignant brain tumor patients (four glioblastoma, one anaplastic astrocytoma) were evaluated. GFAP and EGFR were overexpressed in all five patients. IDH-1 overexpression was not observed in any

Table 2. Clinical Evaluation and Image Results

Group	*Patient no.*	*Pathology*	*Clinical response*	*Progression-free survival (months)*	*Overall survival (months)*	*TNR, ^{99m}Tc-IDA-D-[c(RGDfK)]$_2$*	*meanSUV, ^{18}F-FDG*	*TNR, ^{18}F-FDG*
Lung cancer ($n = 5$)	1	Adenocarcinoma	CR	123	123	2.1	1.4	2.4
	2	Adenocarcinoma	CR	139	139	2.2	6.1	10.3
	3	Adenocarcinoma	PD	6	8	2.9	3.9	8.6
	4	Squamous cell carcinoma	CR	17	17	1.0	1.9	2.0
	5	Sarcomatoid carcinoma	CR	99	99	3.5	7.4	18.7
Brain tumor ($n = 7$)	6	Glioblastoma	PD	34	72	8.7	7.2	1.3
	7	Glioblastoma	PD	16	123	5.5	3.3	1.0
	8	Glioblastoma	PD	8	64	7.5	5.8	1.1
	9	Glioblastoma	PD	6	10	4.6	3.3	1.1
	10	Anaplastic astrocytoma	PD	9	77	2.3	3.1	0.4
	11	Meningioma	SD	134	134	2.3	2.9	0.4
	12	Metastasis (lung, adenocarcinoma)	PD	67	88	13.8	6.1	0.9

CR, complete response; FDG, fluorodeoxyglucose; PD, progressive disease; SD, stable disease; TNR, tumor-to-normal uptake ratio.

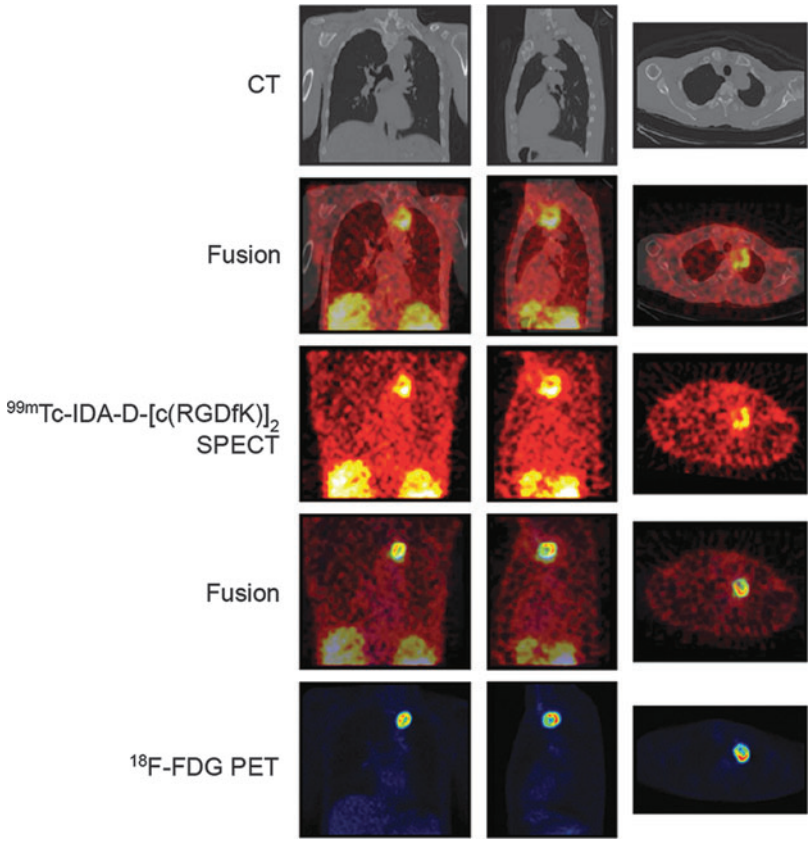

FIG. 1. SPECT and ^{18}F-FDG PET images for a patient with sarcomatoid lung carcinoma. Tumor angiogenesis and tumor metabolism are well visualized on ^{99m}Tc-IDA-D-[c(RGDfK)]$_2$ and ^{18}F-FDG PET images, respectively. Tumor localization corresponds across all images. FDG, fluorodeoxyglucose; PET, positron emission tomography; SPECT, single-photon emission computed tomography.

patients. p53 overexpression was observed in one glioblastoma patient (patient no. 6), and loss of PTEN was observed in three glioblastoma patients (patient nos. 6, 8, and 9). There was no significant correlation between GFAP, IDH-1, PTEN, EGFR, p53 expression status, and TNRs of ^{99m}Tc-IDA-D-[c(RGDfK)]$_2$ SPECT and ^{18}F-FDG PET/CT. However, there was a positive correlation between the Ki-67 proliferation index and TNRs of ^{99m}Tc-IDA-D-[c(RGDfK)]$_2$ SPECT and ^{8}F-FDG PET/CT images (Fig. 4) ($r=0.98$, $p<0.001$, and $r=0.93$, $p<0.01$, respectively).

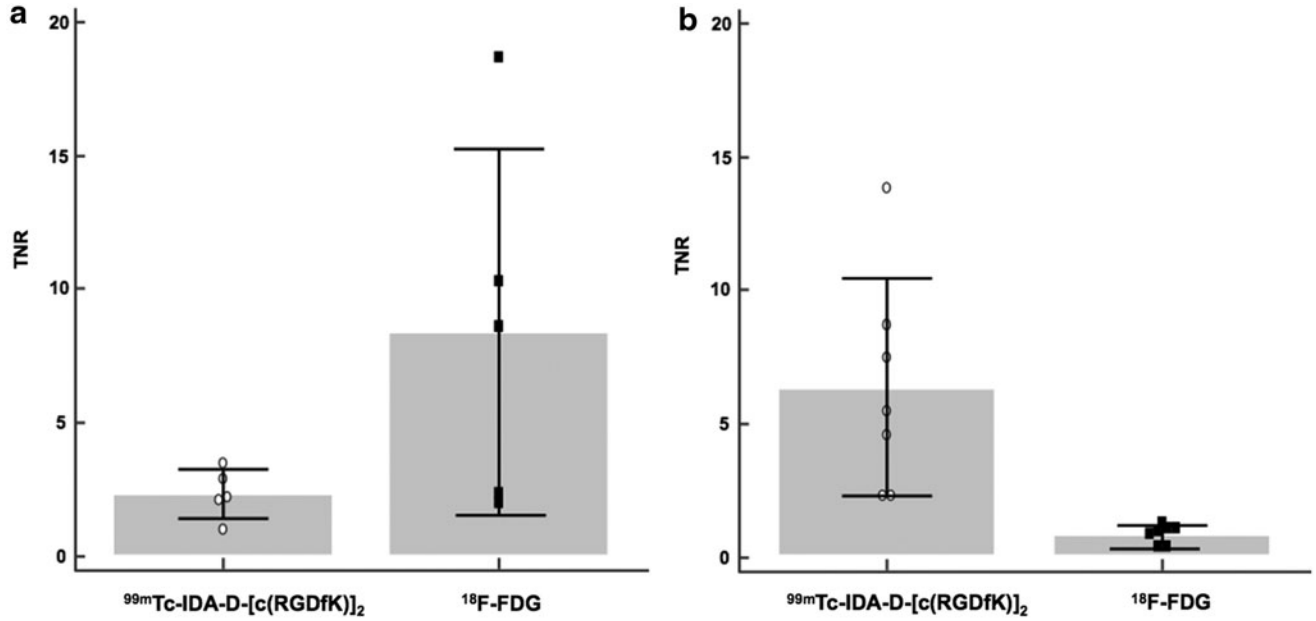

FIG. 2. **(a)** There were no significant differences of TNR values of ^{99m}Tc-IDA-D-[c(RGDfK)]$_2$ SPECT images and ^{18}F-FDG PET/CT images in lung cancer patients. **(b)** TNR values of ^{99m}Tc-IDA-D-[c(RGDfK)]$_2$ SPECT images were significantly higher compared with ^{18}F-FDG PET/CT images in brain tumor patients ($p=0.02$). TNR, tumor-to-normal uptake ratio.

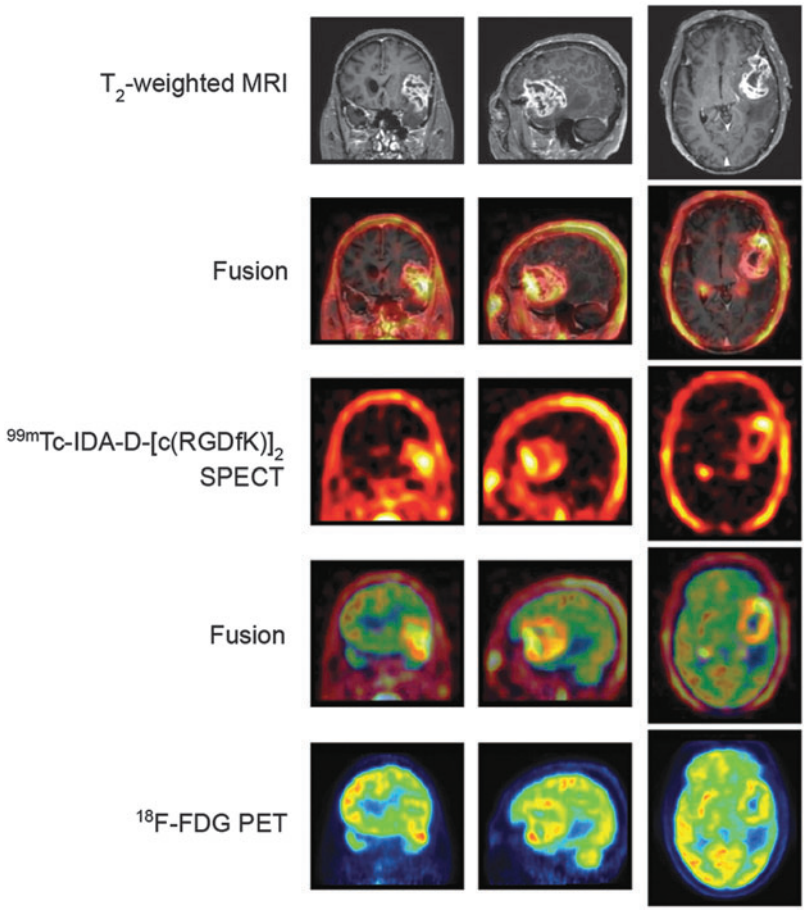

FIG. 3. SPECT and ^{18}F-FDG PET images for a patient with brain glioblastoma. Tumor angiogenesis and tumor metabolism are well visualized on ^{99m}Tc-IDA-D-[c(RGDfK)]$_2$ SPECT and ^{18}F-FDG PET images, respectively. Tumor localization corresponds across all images.

Discussion

In the present study, the authors demonstrated, for the first time in humans as per their knowledge, the clinical efficacy of ^{99m}Tc-IDA-D-[c(RGDfK)]$_2$ SPECT for the visualization and localization of activated angiogenesis in brain and lung tumors. This is also the first RGD peptide targeting SPECT study for brain tumors. Moreover, the authors investigated the relationship between the activation of angiogenesis and altered glucose metabolism in these tumors in an attempt to provide a foundation for a unique application of integrin $\alpha_v\beta_3$-specific imaging. In addition, no adverse event was reported in association with ^{99m}Tc-IDA-D-[c(RGDfK)]$_2$ injection, to conclude that ^{99m}Tc-IDA-D-[c(RGDfK)]$_2$ injection should be safe and well tolerated.

The present clinical study, together with their previous preclinical studies,[17,19] suggests that ^{99m}Tc-IDA-D-[c(RGDfK)]$_2$ SPECT imaging reflects angiogenesis by visualizing integrin

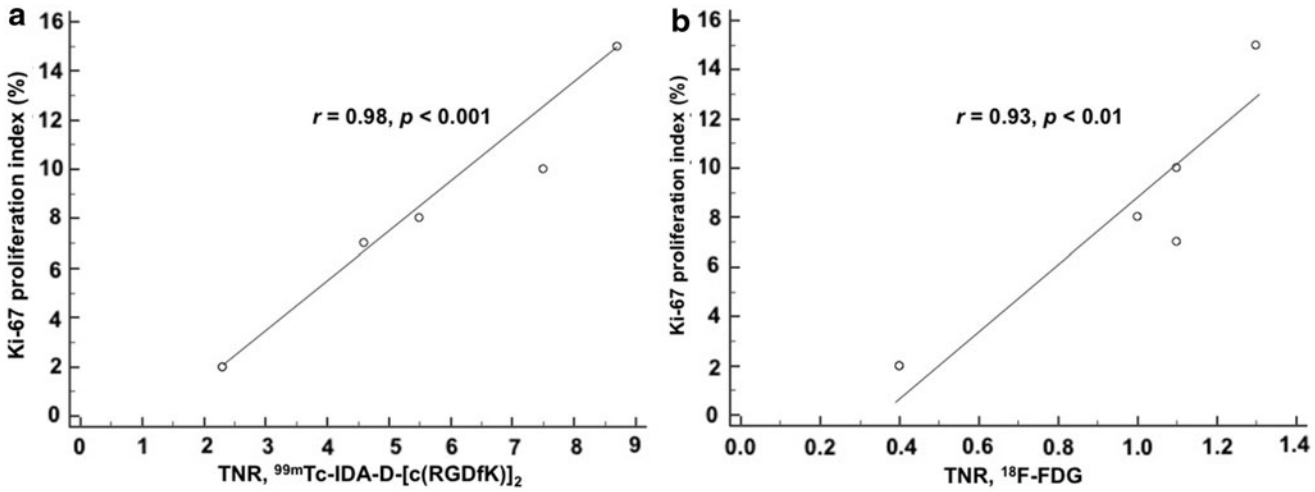

FIG. 4. Positive correlation between the Ki-67 proliferation index and TNRs of **(a)** ^{99m}Tc-IDA-D-[c(RGDfK)]$_2$ SPECT ($r=0.98$, $p<0.001$) and **(b)** ^{18}F-FDG PET/CT ($r=0.93$, $p<0.01$) images.

$\alpha_v\beta_3$ overexpression in both lung cancers and brain tumors. However, the relationship between the level of active angiogenesis and glucose metabolism was different between lung cancers and brain tumors. This was because tumor contrast was more prominent on ^{18}F-FDG PET images than on ^{99m}Tc-IDA-D-[c(RGDfK)]$_2$ SPECT images of lung cancers, while the opposite was true for brain tumors. However, discrepancies in tumor contrast across organs and tracers must be carefully interpreted after considering differences in the metabolic properties or pharmacodynamics of both tracers, regardless of the level of integrin $\alpha_v\beta_3$ expression. While ^{99m}Tc-IDA-D-[c(RGDfK)]$_2$ binds to integrin $\alpha_v\beta_3$ expressed in endothelial cells,[19] ^{18}F-FDG substantially accumulates not only in tumors but also in normal tissues of the brain, thus resulting in a lower TNR value, whereas it accumulates significantly in tumors and negligibly in normal tissues of the lung, resulting in a higher TNR value.

Intense uptake of ^{99m}Tc-IDA-D-[c(RGDfK)]$_2$ by tumors facilitated the clear detection of overexpressed integrin $\alpha_v\beta_3$ on SPECT images of lung and brain tumors in the present study. The authors assessed the clinical efficacy of ^{99m}Tc-IDA-D-[c(RGDfK)]$_2$ SPECT using TNR (tumor contrast), because the detectability (sensitivity and specificity) of overexpressed integrin $\alpha_v\beta_3$ in tumors using *in vivo* imaging with a ^{99m}Tc-labeled radiotracer can be determined with a high target-to-background ratio, particularly for small tumors surrounded by normal tissues that may have nonspecific binding sites.[26,27] The mean tumor uptake of ^{99m}Tc-IDA-D-[c(RGDfK)]$_2$ was twice (TNR = 2.3 ± 0.9) the uptake by homogeneous normal tissue on the contralateral side in patients with lung cancers, whereas it was six times (TNR = 6.4 ± 4.0) the uptake by homogeneous normal tissue on the contralateral side in patients with brain tumor. These differences can be strongly attributed to nonspecific binding of the tracer (background) in normal lung tissue. However in the case of brain tumors, the nonspecific binding of ^{99m}Tc-IDA-D-[c(RGDfK)]$_2$ in the surrounding normal brain tissue is prevented by the blood–brain barrier (BBB), while the uptake in the tumor lesions is suggested to be facilitated by the breakage of BBB,[28] resulting in a higher TNR compared to lung cancers. Galeal uptake of ^{99m}Tc-IDA-D-[c(RGDfK)]$_2$ was higher compared with normal brain tissue (data not shown), suggesting that ^{99m}Tc-IDA-D-[c(RGDfK)]$_2$ does not cross the intact BBB, which is consistent with other previous radiolabeled RGD peptide studies.[9,29] Although the pharmacokinetics of ^{99m}Tc-IDA-D-[c(RGDfK)]$_2$ have not been assessed in humans, substantial accumulation of the tracer in the lung is a possible reason for the relatively low TNR in patients with lung tumors. Thus, in brain tumors, contrast caused by activated angiogenesis in tumors was differentiated from the angiogenesis activity in normal tissues by a high TNR. Because a high TNR value can help in the clear identification and localization of overexpressed integrin $\alpha_v\beta_3$ in a tumor, the diagnostic value of integrin $\alpha_v\beta_3$-targeted imaging can be increased for brain tumors with the use of ^{99m}Tc-IDA-D-[c(RGDfK)]$_2$ SPECT, which was shown to identify activated angiogenesis in solid tumors in the present study.

^{18}F-FDG PET/CT is a well-known imaging tool used in the detection, diagnosis, staging, and treatment response monitoring in various cancers. In contrast, angiogenesis is yet to be evaluated for its usefulness as a tumor biomarker in certain situations, despite the various previous imaging studies with multiple types of RGD peptide labeled radioligands. Therefore in this study, ^{99m}Tc-IDA-D-[c(RGDfK)]$_2$ SPECT images were compared with a previously well evaluated tumor biomarker, ^{18}F-FDG, to seek the future potential of ^{99m}Tc-IDA-D-[c(RGDfK)]$_2$ to be clinically utilized as a tumor biomarker in certain malignancies. However, the authors could not observe a statistically significant relationship between the levels of angiogenesis (^{99m}Tc-IDA-D-[c(RGDfK)]$_2$) and tumor glucose metabolism (^{18}F-FDG) in patients with brain tumors. The significance of correlation was marginal in lung cancers and this could be a result confounded by the higher uptake of ^{99m}Tc-IDA-D-[c(RGDfK)]$_2$ by normal lung tissue, due to the lack of BBB from preventing normal tissue uptake, as in brain tumors. Lung cancers and glioma are both FDG-avid type malignancies, and angiogenesis takes a significant role in the pathological process. Their findings suggest that integrin $\alpha_v\beta_3$ expression measured by ^{99m}Tc-IDA-D-[c(RGDfK)]$_2$ SPECT has different clinical impact according to tumor types, based on the physiologic characteristics of organs. An imaging study reported a strong correlation between ^{18}F-FDG uptake and angiogenesis, which was assayed using immunohistochemical analysis in patients with breast cancer,[30] while another reported that the uptake of a positron-emitting radiotracer for the detection of angiogenesis (^{18}F-galacto-RGD) and that of ^{18}F-FDG were not correlated for malignant lesions.[16] Their results provide further evidence for the association between angiogenic activity and metabolism in tumors. Although the clinical implications of this correlation need larger number of patients and further biological evidence, these were not provided in the present study. Moreover, it is important to realize that integrin $\alpha_v\beta_3$ is now assumed to have positive and negative regulatory roles in angiogenesis, depending on the respective pathology. Therefore, these results should be interpreted with caution. Further studies should be done concerning whether ^{99m}Tc-IDA-D-[c(RGDfK)]$_2$ SPECT can provide information regarding the role of angiogenesis in tumor pathophysiology, and moreover, other indexes such as angiogenesis targeted therapy response monitoring.

IHC analysis revealed a significant correlation between the Ki-67 proliferation index and TNRs of ^{99m}Tc-IDA-D-[c(RGDfK)]$_2$ SPECT and ^{18}F-FDG PET. It has been known that Integrin $\alpha_v\beta_3$ plays a role in the proliferation and invasion in brain tumors, particularly in grade III and IV malignant gliomas.[31,32] Therefore, despite the limitations of their study due to its lack of integrin $\alpha_v\beta_3$ level measurement, a positive correlation between ^{99m}Tc-IDA-D-[c(RGDfK)]$_2$ uptake with proliferation and tumor grade implicates that the integrin $\alpha_v\beta_3$ levels measured by ^{99m}Tc-IDA-D-[c(RGDfK)]$_2$ SPECT may reflect the proliferative pathogenesis of malignant brain tumors. Therefore, the authors suggest that ^{99m}Tc-IDA-D-[c(RGDfK)]$_2$ SPECT has a promising future for the utilization as a pathologic biomarker. While there were no significant relationships between clinical responses and TNRs of ^{99m}Tc-IDA-D-[c(RGDfK)]$_2$ SPECT in lung cancer patients, the one patient who had SD in brain tumor groups had the lowest TNR also supports this feature.

The small sample size and the inclusion of mixed disease subtypes are strong limitations of the present study. Because the pharmacokinetics and pharmacodynamics of ^{99m}Tc-IDA-D-[c(RGDfK)]$_2$ can vary according to the disease

subtype, the results of the present study may not be entirely reliable. Further prospective studies with larger sample sizes and homogenous disease subtypes will provide more accurate information. In addition, further studies in humans for direct correlation of pathologic integrin $\alpha_v\beta_3$ expression with ^{99m}Tc-IDA-D-[c(RGDfK)]$_2$ uptake should be needed. Another limitation is the absence of absolute quantification of SPECT data. Although the authors completed a calibration procedure before study initiation to ensure the validity of the quantified values, the lack of attenuation correction for SPECT data limited us from the usage of direct quantification. Hence, the authors adopted the TNR value, which probably eliminated any error that may have occurred from radioisotope attenuation. The authors assume that the attenuation coefficient for the ipsilateral side was comparable with that for the contralateral side, resulting in compensation by division for the calculation of TNR. Finally, the eventual goal of ^{99m}Tc-IDA-D-[c(RGDfK)]$_2$ SPECT studies would be evaluating the possibility of clinical application, such as grading, metastasis workup, or angiogenesis targeted therapy response monitoring. This would require a future prospective study with a larger cohort of patients.

Conclusion

In conclusion, the authors performed successful SPECT imaging of lung cancers and brain tumors using ^{99m}Tc-IDA-D-[c(RGDfK)]$_2$, which binds to integrin $\alpha_v\beta_3$ that is overexpressed during angiogenesis. The injection of ^{99m}Tc-IDA-D-[c(RGDfK)]$_2$ was safe and well tolerated by patients, without clinically important safety problems. These results demonstrate that ^{99m}Tc-IDA-D-[c(RGDfK)]$_2$ is an efficacious and safe radiotracer for imaging integrin $\alpha_v\beta_3$ expression in lung cancers and brain tumors. Moreover, it may be possible to predict and monitor the clinical efficacy of antiangiogenic agents in malignant tumors using ^{99m}Tc-IDA-D-[c(RGDfK)]$_2$ SPECT.

Acknowledgments

This research was supported by the Korea Health Technology R&D Project through the Korea Health Industry Development Institute (KHIDI), funded by the Ministry of Health and Welfare, Republic of Korea (HI14C1072) and the National Research Foundation of Korea (NRF), funded by the Ministry of Science and ICT, Republic of Korea (NRF-2015R1D1A1A02061707, NRF-2016R1D1A1A02937028).

Disclosure Statement

There are no existing financial conflicts.

References

1. Ferrara N. Role of vascular endothelial growth factor in regulation of physiological angiogenesis. Am J Physiol Cell Physiol 2001;280:C1358.
2. Neufeld G, Cohen T, Gengrinovitch S, et al. Vascular endothelial growth factor (VEGF) and its receptors. FASEB J 1999;13:9.
3. Veikkola T, Karkkainen M, Claesson-Welsh L, et al. Regulation of angiogenesis via vascular endothelial growth factor receptors. Cancer Res 2000;60:203.
4. Gaertner FC, Kessler H, Wester HJ, et al. Radiolabelled RGD peptides for imaging and therapy. Eur J Nucl Med Mol Imaging 2012;39 Suppl 1:S126.
5. Haubner R, Wester HJ. Radiolabeled tracers for imaging of tumor angiogenesis and evaluation of anti-angiogenic therapies. Curr Pharm Des 2004;10:1439.
6. Laverman P, Sosabowski JK, Boerman OC, et al. Radiolabelled peptides for oncological diagnosis. Eur J Nucl Med Mol Imaging 2012;39 Suppl 1:S78.
7. Brooks P, Clark R, Cheresh D. Requirement of vascular integrin alpha v beta 3 for angiogenesis. Science 1994;264:569.
8. Ruoslahti E. Specialization of tumour vasculature. Nat Rev Cancer 2002;2:83.
9. Chen H, Niu G, Wu H, et al. Clinical Application of radiolabeled RGD peptides for PET imaging of integrin alphavbeta3. Theranostics 2016;6:78.
10. Zheng K, Liang N, Zhang J, et al. ^{68}Ga-NOTA-PRGD$_2$ PET/CT for integrin imaging in patients with lung cancer. J Nucl Med 2015;56:1823.
11. Li D, Zhao X, Zhang L, et al. ^{68}Ga-PRGD$_2$ PET/CT in the evaluation of Glioma: A prospective study. Mol Pharm 2014; 11:3923.
12. Knetsch PA, Petrik M, Griessinger CM, et al. [68Ga] NODAGA-RGD for imaging $\alpha v\beta 3$ integrin expression. Eur J Nucl Med Mol Imag 2011;38:1303.
13. Haubner R, Kuhnast B, Mang C, et al. [18F]Galacto-RGD: Synthesis, radiolabeling, metabolic stability, and radiation dose estimates. Bioconjug Chem 2004;15:61.
14. Chen X, Park R, Tohme M, et al. MicroPET and autoradiographic imaging of breast cancer alpha v-integrin expression using ^{18}F- and ^{64}Cu-labeled RGD peptide. Bioconjug Chem 2004;15:41.
15. Mulder WJ, Griffioen AW. Imaging of angiogenesis. Angiogenesis 2010;13:71.
16. Beer AJ, Lorenzen S, Metz S, et al. Comparison of integrin alphaVbeta3 expression and glucose metabolism in primary and metastatic lesions in cancer patients: A PET study using 18F-galacto-RGD and ^{18}F-FDG. J Nucl Med 2008;49:22.
17. Lee BC, Moon BS, Kim JS, et al. Synthesis and biological evaluation of RGD peptides with the ^{99m}Tc/^{188}Re chelated iminodiacetate core: Highly enhanced uptake and excretion kinetics of theranostics against tumor angiogenesis. RSC Adv 2013;3:782.
18. Garcia Garayoa E, Schweinsberg C, Maes V, et al. Influence of the molecular charge on the biodistribution of bombesin analogues labeled with the [^{99m}Tc(CO)3]-core. Bioconjug Chem 2008;19:2409.
19. Yoo JS, Lee J, Jung JH, et al. SPECT/CT Imaging of high-risk atherosclerotic plaques using integrin-binding RGD dimer peptides. Sci Rep 2015;5:11752.
20. Gao S, Wu H, Li W, et al. A pilot study imaging integrin alphavbeta3 with RGD PET/CT in suspected lung cancer patients. Eur J Nucl Med Mol Imaging 2015;42:2029.
21. Schnell O, Krebs B, Wagner E, et al. Expression of integrin alphavbeta3 in gliomas correlates with tumor grade and is not restricted to tumor vasculature. Brain Pathol 2008; 18:378.
22. Alberto R, Schibli R, Egli A, et al. A novel organometallic aqua complex of technetium for the labeling of biomolecules: Synthesis of [^{99m}Tc(OH$_2$)3(CO)$_3$]+ from [^{99m}TcO$_4$]- in aqueous solution and its reaction with a bifunctional ligand. J Am Chem Soc 1998;120:7987.
23. Chen B, Zhao G, Ma Q, et al. (^{99m})Tc-3P-RGD$_2$ SPECT to monitor early response to bevacizumab therapy in patients

with advanced non-small cell lung cancer. Int J Clin Exp Pathol 2015;8:16064.
24. Jin X, Liang N, Wang M, et al. Integrin imaging with ^{99m}Tc-3PRGD$_2$ SPECT/CT shows high specificity in the diagnosis of lymph node metastasis from non-small cell lung cancer. Radiology 2016;281:958.
25. Zhu Z, Miao W, Li Q, et al. ^{99m}Tc-3PRGD$_2$ for integrin receptor imaging of lung cancer: A multicenter study. J Nucl Med 2012;53:716.
26. Zhao D, Jin X, Li F, et al. Integrin alphavbeta3 imaging of radioactive iodine-refractory thyroid cancer using ^{99m}Tc-3PRGD$_2$. J Nucl Med 2012;53:1872.
27. Zhou Y, Chakraborty S, Liu S. Radiolabeled cyclic RGD peptides as radiotracers for imaging tumors and thrombosis by SPECT. Theranostics 2011;1:58.
28. Wolburg H, Noell S, Fallier-Becker P, et al. The disturbed blood-brain barrier in human glioblastoma. Mol Aspects Med 2012;33:579.
29. Schnell O, Krebs B, Carlsen J, et al. Imaging of integrin alpha(v)beta(3) expression in patients with malignant glioma by [18F] Galacto-RGD positron emission tomography. Neuro Oncol 2009;11:861.
30. Groves AM, Shastry M, Rodriguez-Justo M, et al. ^{18}F-FDG PET and biomarkers for tumour angiogenesis in early breast cancer. Eur J Nucl Med Mol Imaging 2011;38:46.
31. Veeravagu A, Liu Z, Niu G, et al. Integrin alphavbeta3-targeted radioimmunotherapy of glioblastoma multiforme. Clin Cancer Res 2008;14:7330.
32. Onishi M, Ichikawa T, Kurozumi K, et al. Angiogenesis and invasion in glioma. Brain Tumor Pathol 2011;28:13.